Available online at www.sciencedirect.com
ScienceDirect
Journal of the European Ceramic Society 28 (2008) 2421–2431
www.elsevier.com/locate/jeurceramsoc

Lanthanum phosphate calcium aluminate glasses: ^{27}Al and ^{31}P NMR spectroscopy

R. Marzke [a,*], S. Boucher [b], G. Wolf [b], J. Piwowarczyk [a], W. Petuskey [b]

[a] *Department of Physics and Astronomy, Arizona State University, Tempe, AZ 85287-1504, USA*
[b] *Department of Chemistry and Biochemistry, Arizona State University, Tempe, AZ 85287-1604, USA*

Available online 3 June 2008

Abstract

A new protocol for synthesis of glassy aluminates with substantial content of the refractory compound $LaPO_4$ has been developed, utilizing hydrated monazite and anhydrous metal oxides as starting materials. Ultra high-temperature NMR of samples containing up to 75 mol% $LaPO_4$ shows that monazite is incorporated homogeneously into melts, while analysis by electron microprobe, X-ray diffraction, solid-state NMR and Raman scattering shows that water quench of samples with 50% La–monazite or less results primarily in glass formation. Network structures of the $LaPO_4$-containing glasses remain aluminate-based, as indicated by our samples' melting points (>1200 °C), well above those of phosphate glasses. Melting temperatures exhibit a minimum in the range 20–30% $LaPO_4$ content. Raman spectra show only isolated phosphate groups, with no P–O–P bonds (orthophosphates). Dissolution observations, electron microprobe composition measurements and a substantially shifted principal ^{31}P NMR line show that La^{3+} lies within the second coordination shell around P in all of the glasses. P–Al TRAPDOR NMR studies and a second, more negatively shifted line in the ^{31}P spectra indicate that P is also closely coordinated to one or two Al ions.

Keywords: Spectroscopy; Al_2O_3; Glass; Thermal properties; NMR

1. Introduction

1.1. General

The glass-forming ability and crystallization characteristics of phosphates and aluminates have given rise to renewed interest in these materials, as have their thermal and IR transmission properties.[1–3] For example, phosphate glass use in optical components is increasing, and for this the glasses are stabilized by the addition of alumina.[4,5] Aluminates figure prominently in several scientific and engineering applications, for example as support structures for optically active components in electronic systems.[2] Doping of both phosphate and aluminate glasses with rare earth elements allows tuning of the fluorescence of those elements.[2,6]

Among materials for high-temperature applications, the refractory compound lanthanum–monazite ($LaPO_4$) has been intensively investigated because of its potential usefulness in composites with alumina fibers in extreme environments.[3,7] However, systems containing aluminates combined with $LaPO_4$ have not been widely studied. In pursuit of this goal, we developed a novel synthesis approach for the ternary system alumina, calcia and La–monazite, with monazite concentrations ranging from 12 to 75 mol%. Samples were examined initially in the liquid phase via ultra high-temperature ^{27}Al NMR, and then were investigated in the solid phase by ^{31}P and ^{27}Al NMR as well as Raman scattering.

Liquid-phase NMR requires melting of a ~3 mm diameter sample using a CO_2 laser while levitating the sample in an NMR spectrometer, in a stream of argon gas or air.[8–10] Results for the liquid state of La monazite-containing samples have been discussed elsewhere.[9,11,12] A consistent finding has been the observation above melting of a single narrow ^{27}Al NMR line, with a well-defined chemical shift that varies with La–monazite content. This shows that the molten state is characterized by a homogeneous Al chemical and structural environment. A second finding has been that following water quench a large fraction of the resulting samples are glassy, especially for starting $LaPO_4$ concentrations below 50%. Our extended studies of these glassy samples are the subject

* Corresponding author.
E-mail address: Robert.Marzke@asu.edu (R. Marzke).

0955-2219/$ – see front matter © 2008 Elsevier Ltd. All rights reserved.
doi:10.1016/j.jeurceramsoc.2008.03.023

Table 1
Selected information on the pure calcium aluminates used in this study[8,14]

Common nomenclature[a]	Formula	$CaO:Al_2O_3$	T_m (°C) (anhydrous)	Notes
C12A7	$Ca_{12}Al_{14}O_{33}$	1:0.58	1415	Cools to glass, is reactive contaminant of cements
CA	$CaAl_2O_4$	1:1	1602	Readily cools to glass, is used in "calcium aluminate" cement

[a] Industrial ceramic and cement industry usage derives from abbreviations of the raw manufacturing ingredients.

of this paper. Answers to two principal questions have been sought. These are: (1) what is the nature of the networks in these new glasses, which are produced from compounds that belong to two powerful glass forming families, aluminates and phosphates? (2) What are the relative locations of ions within their networks? We begin with a description of the samples' synthesis.

2. Methods—synthesis and characterization

2.1. Synthesis—background

Synthesis of glassy materials involving phosphates is generally carried out in sealed platinum crucibles, using phosphate compounds as starting materials.[4,5] The crucible is heated to the expected melting point of the sample and then rapidly quenched. To meet our initial requirements for NMR samples in the form of spherical beads for levitation, however, required use of an image furnace, which melts a rod-shaped parent sample in the presence of a flowing gas such as nitrogen. This can be problematic in samples containing phosphorus, which reacts with water to form compounds that vaporize readily at elevated temperatures.[13,14] Fortunately for image furnace applications, however, lanthanum phosphate is insoluble and non-reactive at moderate temperatures and in aqueous solutions.[15] The compound is readily available commercially, and we set out to develop a synthesis protocol that would allow the production of gram quantities of monazite-containing samples, exposed to air at temperatures in excess of 1400 °C.

For starting materials in the calcia–alumina family, calcium aluminates provided convenient choices. Extensive data have been compiled on calcium aluminate solid forms, both hydrous and anhydrous.[16,17] There are five common anhydrous compounds, all stable at standard pressure, temperature, and 50% relative humidity. The two we found most suitable for this study have the common abbreviated names CA and C12A7, as listed in Table 1.

Synthetic protocols for CA and C12A7 that do not go through a melt phase produce mixtures containing significant amounts of other calcium aluminate compounds, all in mutual contamination.[15,16] These compounds differ in the stoichiometry of CaO to Al_2O_3, as well as in their reactivity and physical properties. The components of this system must be melted to form any homogeneous phases, either glass or crystalline.[15,16] Also, calcium aluminates and lanthanide phosphates are avid binders of large quantities of atmospheric water, which was taken into consideration while developing the synthesis method.[15,16]

$LaPO_4$ was added to the samples by mixing 99.99% pure $LaPO_4{\cdot}5H_2O$[b] powder with the appropriate CA or C12A7 base material, just prior to packing into the rod-forming mold. Calcining $LaPO_4{\cdot}5H_2O$ in advance yields poor and variable results. These included significant loss of phosphorus, probably due to chemical reactions between the phosphate, oxygen and formula water in the calcined powder at high temperatures. An example of a reaction series that could lead to this loss is

$$LaPO_4{\cdot}5H_2O \rightarrow H_3PO_4 + La(OH)_3{\cdot}2H_2O$$

$$4H_3PO_4 \rightarrow 6H_2O + P_4O_{10}\uparrow \quad T_{sub} = 362\,^{\circ}C$$

Surprisingly, the use of $LaPO_4$ powder in its hydrous form, when added to completely dry, pre-sintered C12A7 or CA-based material, yielded acceptable results. (Powder X-ray diffraction analysis of the commercial lanthanum phosphate, prior to use, affirmed a stoichiometry of $LaPO_4{\cdot}5H_2O$.) As discussed below, we believe this was due to the high affinity and rapid binding of the aluminates with water, removing it from access to the phosphate before any appreciable reaction could take place. Gram quantities of $LaPO_4$-containing samples could thus be prepared in air without the need for expensive sealed platinum crucibles. Both series of samples experienced temperatures up to 1400 °C under air and/or nitrogen without apparent decomposition. Following establishment of the use of hydrated $LaPO_4$, full sample production was implemented as set forth in the next section.

2.2. Synthesis technique

A bulk preparation containing CaO and $Ca(OH)_2$[c] was calcined overnight at 600 °C before use, then powdered, resulting in anhydrous CaO (see Fig. 1). Al_2O_3[d] was also calcined overnight at 600 °C to remove adsorbed water. These two oxides were pulverized and mixed in a ball mill in stoichiometric proportions for either C12A7 or CA. Both materials were at least 99% pure.[e] The powders were transferred into alumina crucibles and sintered at 1450 °C. The sintered material was re-pulverized, and re-sintered several times until X-ray diffraction patterns revealed the loss of all original end member compounds. $LaPO_4$ hydrate was then added as required for each desired formulation, taking account of water of hydration, and the mixtures were sintered once again. Sintering of the $LaPO_4$-containing mixtures required

[b] Alza.
[c] J.T. Baker.
[d] Mitutoyo Chemical Co., Tokyo.
[e] Electron microprobe revealed approximately 0.5% silicon as the major impurity, also 0.2% titanium. No detectable iron was found.

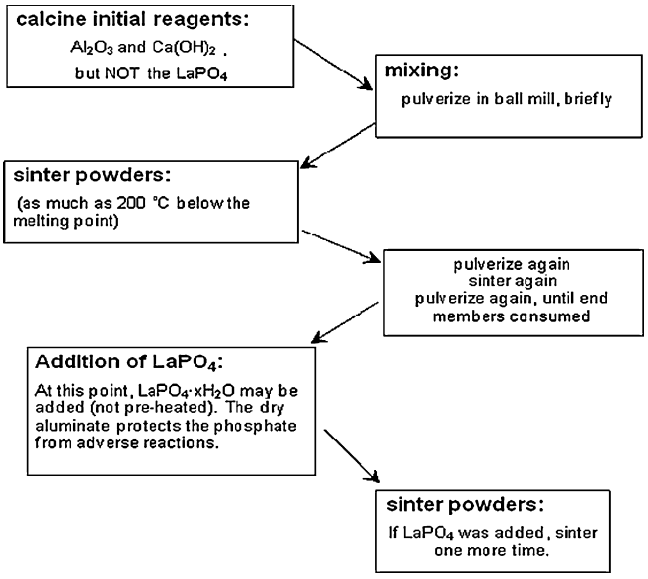

Fig. 1. Initial procedures in sample synthesis.

Table 2
Sintering and melting temperatures of samples

$LaPO_4$ (%)	Sintering/melting temperature in CA (°C)	Sintering/melting temperature in C12A7 (°C)
0	1375/1600	1375/1415
12.5	u.d./u.d.	1280/1320
20	1180/1225	1255/1300
25	1230/u.d.	1230/1275
50	1350/u.d.	1350/1450
75	1398/1550	1398/1450

u.d.: undetermined.

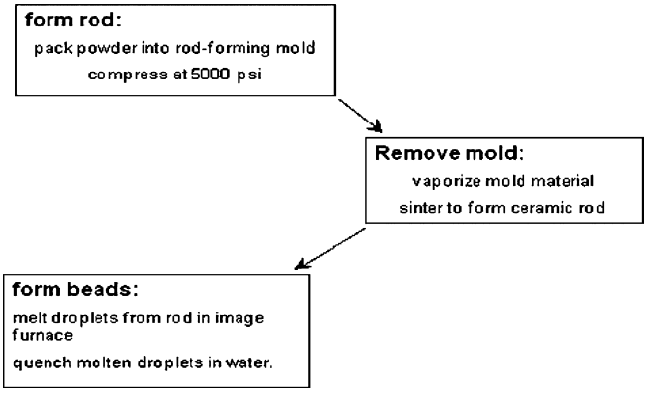

Fig. 2. Final sample preparation.

different temperatures from those used for the pure ceramic base materials (see Table 2 and melting point discussion). In all samples powder X-ray diffraction patterns taken at this stage reveal a complex mixture of many calcium aluminate variants.

The next steps in sample preparation (Fig. 2) were packing the multi-compound powder into a rod-forming cold press[f] and compressing at 5000 psi, then performing a final sintering at an appropriate temperature several hundred degrees below melting (see Table 2). The result was a firm, porous crystalline ceramic rod, still containing multiple coexisting compounds. The rod was transferred to an image furnace[g] and heated until droplets melted off, which passed through a coarse Pt screen, and were quenched in ultra-pure water. Spheroidal beads with diameters from 2 to 4 mm were formed, having either crystalline or glassy character and uniform aluminate content corresponding either to C12A7 or to CA. For initial $LaPO_4$ fractions below 75%, more than half of the samples were glassy. Microprobe analysis and X-ray powder diffraction studies of many samples gave exact final proportions of lanthanum and phosphorus.

Because of the drop quench, significant quantities of water could conceivably have been entrained in the beads, resulting in CA or C12A7 hydrates. Characterization of the samples, however, showed that they were mainly anhydrous. This is discussed further in Section 4.

2.3. Melting point determination

During synthesis of both CA and C12A7 series the sintering the temperature of the monazite-containing samples had to be altered, in order to accommodate lower melting points. Each new composition was first attempted under the sintering conditions of a previous sample. After retrieval of the material from the sintering oven, visual observation of the sample readily determined that full melting had taken place during the heating process. Another sintering was then attempted at a temperature 25 °C lower than the previous trial. The lowest temperature at which complete melting was observed was recorded as the melting point (T_m) for that composition. Accuracy for the T_m is thus at best only ±25 °C. Melting point determination was not in itself a goal of this study, so no further effort to refine accuracy was attempted, but the relatively high (>1200 °C) values of T_m for all samples were evident.

2.4. Characterization—differential thermal analysis

The glass transition temperatures of the glassy samples were monitored by differential thermal analysis (DTA) on a PerkinElmer thermal analyzer in the Goldwater Materials Science Laboratory at Arizona State University. The sample was heated at 2 °C/min in a platinum crucible under a helium atmosphere, and results for C12A7 and CA were in agreement with literature values, to within ±10 °C. As with melting points, detailed glass temperature studies were not primary goals of this work, but observations of the glass transition along with its temperature were important to understanding the nature of our samples. Representative glass temperatures are given in Table 3 in the next section, along with composition and melting points.

[f] Depths of the Earth, Cave Creek, AZ.

[g] NEC, Tokyo, Japan.

Table 3
Composition results and selected properties of the calcium aluminate:$LaPO_4$ glasses

Glass	Composition by microprobe		T_g (°C)	T_m (°C) crystal	^{27}Al (liq) NMR δ	^{27}Al (sol) NMR δ	^{31}P (sol) NMR δ	Notes
	$CaO:Al_2O_3$	$LaPO_4$ (%)						
CaO	1:0	0	N.A.	2572	N.A.	N.A.	N.A.	
C12A7	12:7.0	0	850[25], 874[8,22]	1415	86	77	N.A.	
C12A7:12% $LaPO_4$	12:7.1	11.2	N.A.	1320 (20%: 1300)	N.A.	N.A.	2/−4	
C12A7:25% $LaPO_4$	12:7.0	20.6	837	1275	85	71	2/−4	
C12A7:50% $LaPO_4$	12:7.1	47.1	812	1450	72	10	2/−4	X-ray traces of $Ca_3La(PO_4)_3$
C12A7:75% $LaPO_4$	12:7.0	63.0	N.A.	N.A.	71	N.A.	0/−3/−6	X-ray traces of $Ca_3La(PO_4)_3$, bright zones of $Ca_3La(PO_4)_3$ dark zones: C12A7, 63% $LaPO_4$
CA	1:.9	0	905[8,22]	1600	76	68		
CA 25% $LaPO_4$	1:1	25.2	N.A.	(20%) 1225	78	66	2/−4	
CA 50% $LaPO_4$	1:.9	46.7	N.A.	N.A.	72	57	2/−4	X-ray traces of $LaPO_4$ (microcrystalline)
CA 75% $LaPO_4$	1:1	72.6	N.A.	1550	72	N.A.	2/−4	X-ray traces of $LaPO_4$ (microcrystalline)
$LaPO_4$	0	100	N.A.	2072	N.A.	N.A.		

Concentration notation for the C12A7, samples: Electron microprobe-measured metal fractions for the sample labeled 50% $LaPO_4$ in C12A7 are: 25 La, 25 P, 22 Ca, 28 Al (at.%). Starting percentages differ from these by less than 5. To convert to ternary phase diagram end members, C12A7 50% $LaPO_4$ would be: 50 $LaPO_4$, 32 CaO, 18 Al_2O_3 (mol%).

2.5. Characterization—electron microscopy

Electron micrographs gave the first evidence that the samples obtained were glassy, even for compositions up to 50% $LaPO_4$ in both C12A7 and CA series. It was found in SEM images that phase separation does not occur frequently in the rapidly quenched samples (Fig. 3A below). Slower quenching, typically performed by cooling a molten sample used for high-temperature NMR studies in a stream of Ar gas, results in nearly complete phase separation (Figs. 3B and 4). However, for both series the 75% $LaPO_4$ composition (Fig. 5) was difficult to obtain as a spherical glassy bead, requiring repeated attempts at rapid quenching of melts with cold water. Powder diffraction of even the most amorphous 75% samples shows some microcrystalline $LaPO_4$ (and/or $Ca_3La(PO_4)_3$).[18]

It is generally more difficult to obtain glass beads in the C12A7 system. The CA system, with its lower proportion of network-modifying calcium, was more lenient, as borne out by the relative ease of glass bead production. Since alumina and $LaPO_4$ do not mix atomically but instead segregate upon solidification,[9] it appears that Ca in these samples acts to promote glass formation.

2.6. Verification of composition

The chemical composition and structure of the final product was monitored by electron microprobe and X-ray powder diffraction, in addition to Raman scattering and solid-state NMR as described below. Different quench rates were utilized in various experiments, from the very slow rate of <700 °C/sc for molten NMR samples, to the moderate rate of >2000 °C/s in water. As noted above, the slowest rates were seen to allow sufficient time for complete crystallization of $LaPO_4$ from the melt. Also, microprobe analysis and scanning electron micrographs show that samples quenched on long time scales have up to 100% ex-solution of the $LaPO_4$ into the aluminate grain boundaries. No signs of crystallization were visible in glassy samples, however, when they

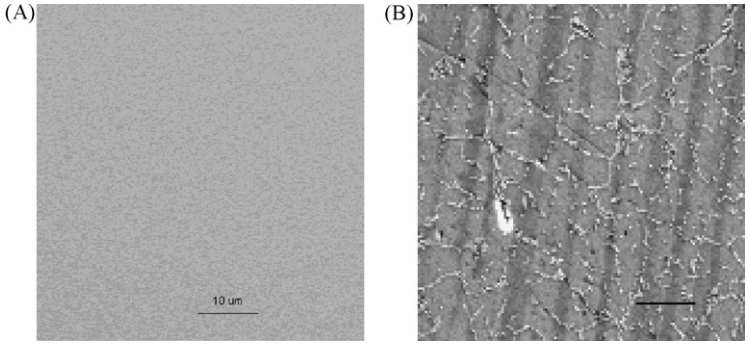

Fig. 3. Microprobe images of quenched 25% $LaPO_4$ in C12A7. (A) Section of a glassy, rapid-quenched sample before NMR analysis. Total width shown: ∼50 μm. (B) Section of a sample that was not quenched rapidly enough, allowing recrystallization of the $LaPO_4$. The bar represents 10 μm. The bright dots are $LaPO_4$. Dark stripes are an artifact.

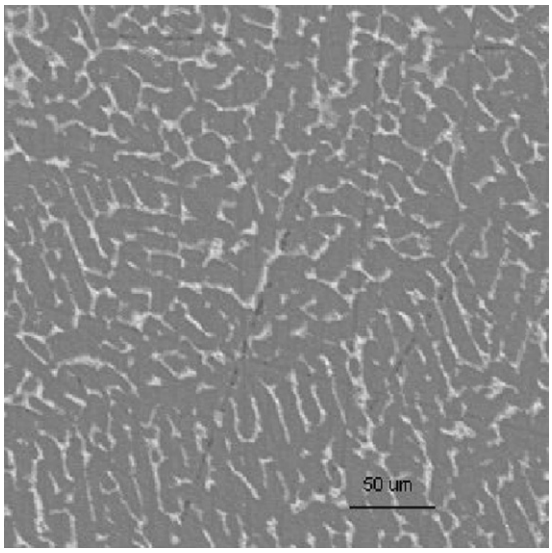

Fig. 4. Microprobe image of 25% $LaPO_4$ in CA. This is a typical sample after a very slow quench (∼700 °C/min), allowing extensive recrystallization and phase separation.

were kept in a desiccator at room temperature over long periods.

2.7. Phosphate dissolution in water and microprobe preparation

The samples were initially prepared for microprobe analysis by embedding in epoxy, and were ground to a very fine polish on silicon carbide sand paper. Since *crystalline* $LaPO_4$ is insoluble in water,[15] water was initially used as the polishing lubricant. The surface of the samples was exposed to water for approximately 1 h during this preparation. Microprobe results, however, revealed a complete loss of phosphate from these samples, presumably owing to the solubility of phosphate *glass* in water.[5,8,19] They also revealed that La was lost in exact proportion to phosphate, as discussed later. The preparation was then repeated using mineral oil as the lubricant.

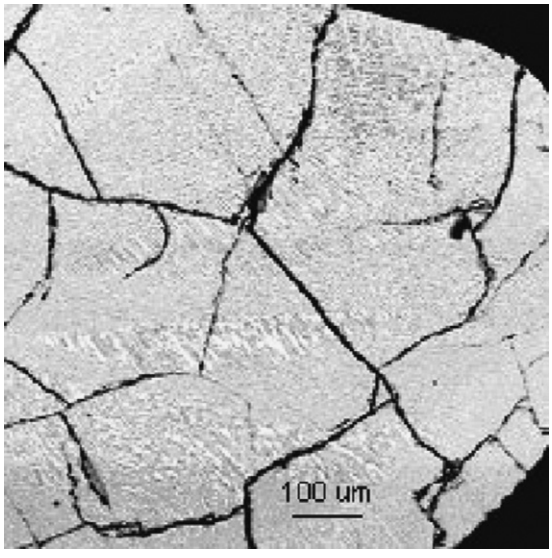

Fig. 5. Microprobe image ("comp mode") of a CA-series sample with high $LaPO_4$ content (75%), post-drop-quench. Significant phase and composition separations and some crystalline character are apparent, even though the X-ray diffraction pattern showed only amorphous background.

2.8. NMR acquisition conditions

All of the NMR experiments were carried out on a Varian solids 300 MHz spectrometer at a field of ∼7 T, with Larmor frequencies of 78.2 MHz for ^{27}Al and 121 MHz for ^{31}P. ^{27}Al aluminum chemical shift values are referenced to Al^{3+} in solutions of saturated $Al(NO_3)_3$. Acquisitions of NMR free induction decays (FIDs) for ^{27}Al were performed using a magic angle spinning (MAS) probe, with typical spectrometer settings of 50 kHz bandwidth, ∼300 W r.f. pulse power, 10 Hz pulse repetition frequency, 4096 point acquisition length and ∼12 μs 90° r.f. pulse length. Rapid ^{27}Al spin-lattice relaxation, due to substantial Al quadrupole coupling, has been observed at all temperatures.[11,12] The error in chemical shift for solid ^{27}Al samples, spun at 6.5 KHz, was of order ±1 ppm.

^{31}P NMR measurements were performed on the Varian 300 MHz spectrometer using the same probe, in addition to solid-sample static measurement following slow cooling from the melt in the ultra high-temperature NMR probe. For ^{31}P the standard reference was 85% H_3PO_4 in water, and the spin rate was 6.5 kHz.

2.9. TRAPDOR NMR[20]

TRAPDOR[h] measurements of ^{31}P and ^{27}Al were obtained on the same NMR spectrometer used for the chemical shift determinations, in a MAS rotor with a triple-resonance probe at a rotation speed of 4 kHz. The NMR resonance frequency was approximately 121 MHz for ^{31}P and 78 MHz for ^{27}Al. Two aluminum RF pulse power settings were used, 329 and 640 W. The ^{31}P pulse length required for a $\pi/2$ rotation of the magnetization was 17.5 μs. The duration of the ^{27}Al pulse ranged from 1 to 5 ms. These times correspond to 4–20 rotations of the MAS probe. The TRAPDOR effect increases with increasing ^{27}Al pulse length. Five milliseconds appear to give the maximum effect. Signals were averaged over 128 acquisitions.

The sample was first run without the ^{27}Al pulse, and then repeated with ^{27}Al irradiation. The data were analyzed in the usual manner by subtracting the ^{27}Al-pulsed peak area (S) from the non-^{27}Al-pulse peak area (S_0), and dividing the result by S_0.

2.10. Raman settings

Raman scattering measurements were made using a Jobin-Yvon Triax 550 spectrograph and a Princeton Instruments S.A. intensified diode array detector. The Raman scattering was excited by the 487.9 nm line of a coherent Innova 90-5 Ar^+ laser.

[h] TRAPDOR refers to "transfer of population via double resonance", a solid-state NMR technique that allows monitoring of the degree of proximity of pairs of different nuclei such as Al and P.[20,21]

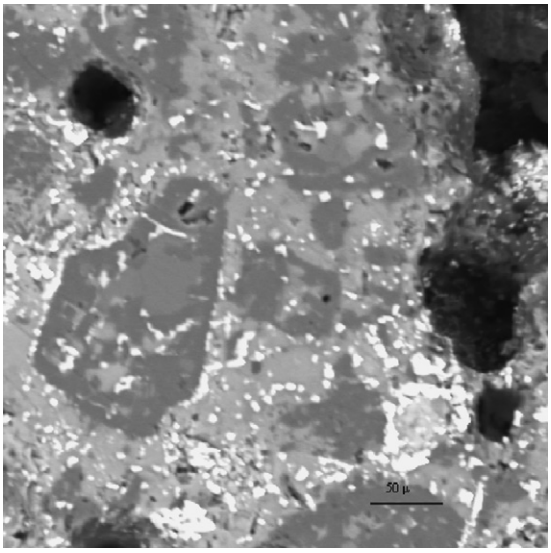

Fig. 6. Microprobe image of sintered 25% $LaPO_4$ in C12A7-based material (prior to melting). The bright areas are $LaPO_4$, The gray regions are grains of calcium aluminate of varying composition (containing no $LaPO_4$).

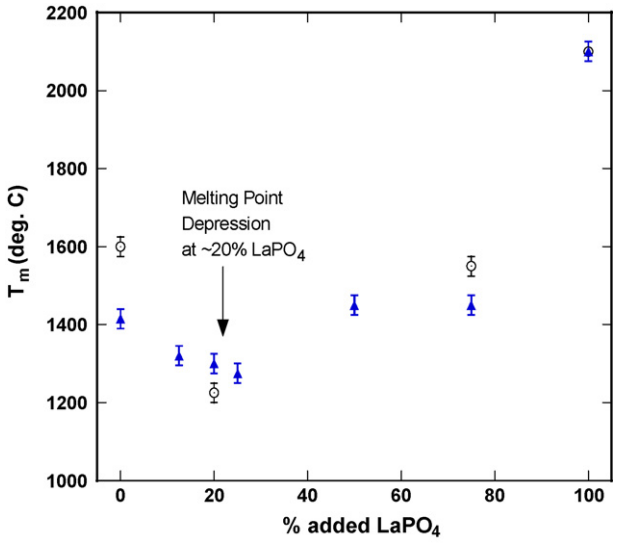

Fig. 7. Melting point changes with composition. Both sample series show a dramatic drop in T_m with added $LaPO_4$.

The scattered radiation was collected through a long-working distance 50× Mitutoyo objective in a modified Olympus BH-2 microscope. The spectra for this study were all averaged over five separate 60 s scans. Raman data on glassy material presented here are from the depolarized mode.

3. Results

3.1. Findings from synthesis and electron microscopy

3.1.1. $(1-x)C12A7{:}xLaPO_4$

$LaPO_4$ does not react with the refractory C12A7 material on sintering. X-ray powder diffraction of sintered samples always reveals the presence of crystalline $LaPO_4$ and various crystalline calcium aluminates. Microprobe analysis of sintered samples shows isolated 'islands' of $LaPO_4$ in the midst of the *multi-crystalline* ceramic, as seen in Fig. 6. However, on further heating, the $LaPO_4$ does dissolve or disperse into the ceramic *melt*, as evidenced in Fig. 3B by the disappearance of the large islands of $LaPO_4$ in beads of quenched melt (both crystalline and glass).

After bead formation in the image furnace, electron micrographs of the fraction of beads that are crystalline show $LaPO_4$ as small ~0.1 μm grains, between the boundaries of calcium aluminate grains. Microprobe measurements show that no calcium or aluminum is present in the $LaPO_4$ grains of these beads.

In the amorphous beads there are no regions of crystallized pure $LaPO_4$, i.e. the structure of the beads prior to image furnace melting appears by electron microscopy as well as X-ray diffraction to be 100% glass, as in Fig. 3A. There was however the unexpected formation of the compound calcium lanthanum phosphate, $Ca_3La(PO_4)_3$ (T_m 1890 °C),[18] weakly observable by X-ray powder diffraction with the 50% sample and clearly present in 75% $LaPO_4$ material. These observations were corroborated by microprobe. In the 25% sample group it was not detected. Microprobe measurements, combined with the absence of an X-ray pattern for the double phosphate $Ca_3La(PO_4)_3$, indicate that for 25% $LaPO_4$ monazite is atomically mixed with C12A7. Upper limits on $LaPO_4$-content values for such mixing are apparently just exceeded in the 50% sample. The presence of any of the calcium phosphate compounds of the apatite family was never observed by X-ray diffraction analysis, pre- or post-melt.

3.1.2. $(1-x)CA{:}xLaPO_4$

As with the C12A7 series, $LaPO_4$ did not react or mix on initial sintering. Also, $LaPO_4$ was incorporated into the amorphous material during melting. Again, no calcium phosphate compounds of the apatite family were observed. However, in contrast to C12A7, no traces were found of calcium lanthanum phosphate, $Ca_3La(PO_4)_3$ in this series.

3.2. The networks: changes in melting point with composition

We now turn to results that bear directly on the nature of the glass network in both series of samples, starting with their melting trends. It was apparent during sample production that the melting points were within the range of aluminate glasses and well above those of phosphate glasses. At lower $LaPO_4$ compositions, both sample series display a minimum melting temperature, as shown in Fig. 7, along with the steep rise in melting that must occur above 75% $LaPO_4$. The position of the minimum is estimated at 25% (±10%) $LaPO_4$ for the C12A7 series and at 20% (±10%) $LaPO_4$ for the CA series.

These melting point findings may be incorporated into a ternary diagram for the entire Al_2O_3–CaO–$LaPO_4$ system as shown in Fig. 8, which includes data from other sources.

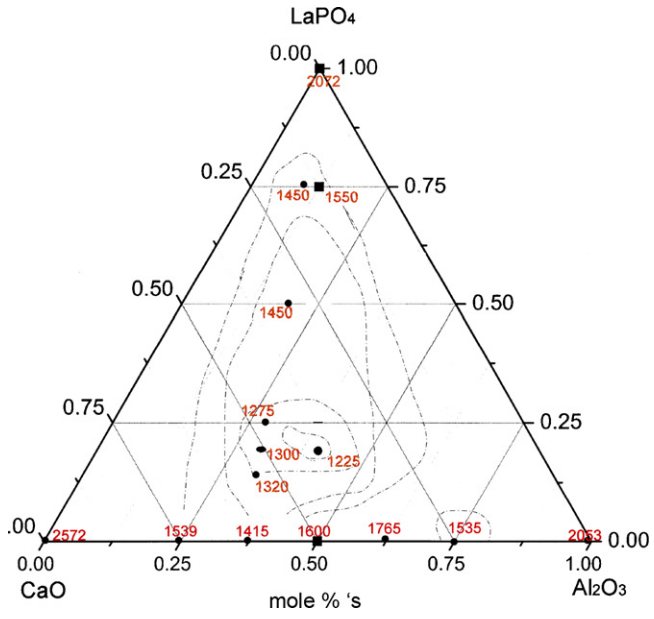

Fig. 8. Modified ternary diagram of the CaO–Al_2O_3–$LaPO_4$ system showing melting points (°C). Data are taken from this work and others.[8] Dashed lines are hand drawn curves of constant melting temperature.

3.3. Raman results

3.3.1. C12A7 samples

The Raman scattering spectra for the solid glassy samples of the C12A7 series are shown in Fig. 9, while those of the CA series are given in Fig. 10.

3.3.2. CA samples

As seen in the figures, CA and C12A7 series' Raman spectra resemble one another and show similar progressions with increasing $LaPO_4$ content. The broad aluminate bands at 556 and ~800 cm^{-1} of the pure compounds[22] quickly disappear, leaving almost no clearly distinguishable indicators of networked aluminate at higher wave numbers, the band near 650 cm^{-1} being attributable to octahedral aluminate formed as a result of disruption of the network by $LaPO_4$. Phosphate manifests its presence

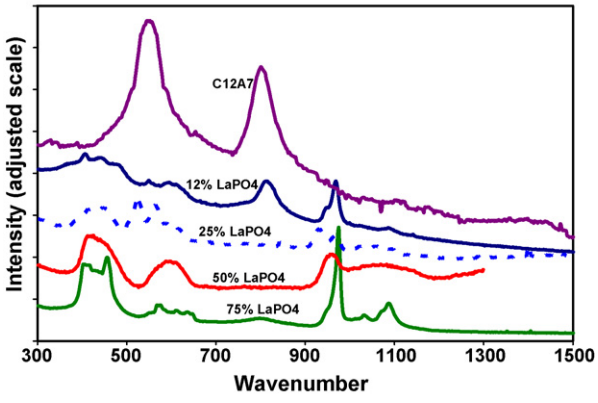

Fig. 9. The depolarized Raman spectra of glassy samples of $(1-x)$ C12A7:$x$$LaPO_4$. The 75% $LaPO_4$ sample contained crystalline phases, including La–monazite, as noted above.

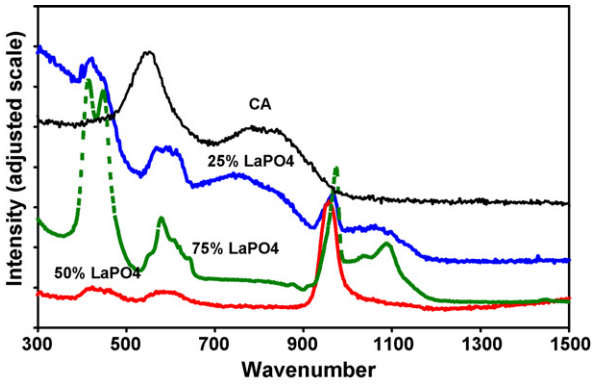

Fig. 10. Raman spectra of samples $(1-x)$CA:$x$$LaPO_4$, calcium monoaluminate (CA) glasses with varying percentages of $LaPO_4$.

strongly, giving rise to a band in the vicinity of 966 cm^{-1}, the symmetric OPO stretch region of the PO_4^{3-} ion. There are also weaker, complex bands at higher wave numbers, again due to phosphate. Notably absent, however, is any indication of Raman scattering from 700 to 800 cm^{-1}, the range of POP vibrations arising from intertetrahedral phosphate–phosphate linkages of Q1 or Q2 phosphate groups. This means that essentially all of the phosphate in the samples is Q0, i.e. the samples have no bridging oxygen and in phosphate glass terminology would be considered orthophosphates. Thus Raman scattering shows that phosphate is intercalated into the network as individual, isolated PO_4 units without intertetrahedral oxygen bridges, leaving the network essentially aluminate, as indicated by the high melting points.

Because concentration increments of $LaPO_4$ were large in this study, evolution of Raman spectra with $LaPO_4$ content could not be followed in detail. The bandwidths all had multiple contributing factors. Small differences in dependences on $LaPO_4$ content are seen in the two series' Raman spectra, which is not surprising in view of differences in the networks' disruption by lanthanum as a cation modifier. C12A7 already has a large excess of modifier, so that the addition of lanthanum only contributes to further network breakup. However, CA has a nearly intact network, consequently requiring more lanthanum to significantly disrupt it.

Disappearance of the 556 cm^{-1} band indicates loss of corner linkages in the aluminate network. Disappearance of the 800 cm^{-1} band, as noted above, indicates even more substantial network disruption. Octahedral aluminate species, to which the band at 650 cm^{-1} is attributed, are not usually observed in Raman scattering, but their presence is expected at higher $LaPO_4$ content from our ^{27}Al NMR results (see below). In such mixed aluminum coordination environments the octahedral Raman band may be present in association with lattice modes,[8] as appears to be the case here. While the low (<400 cm^{-1}) energy bands of glasses are clearly an overlapped sum of multiple sources, one of those sources is probably the Ca–O bond.

Amorphous materials show broad bands, rather than sharp peaks, by Raman spectroscopy. This technique is very sensitive, however, to the presence of ordered material, even when not detectable by X-ray diffraction. A few of these samples, amor-

phous by X-ray diffraction, show that some degree of ordering of atoms had taken place before Raman analysis.

In summary, results viewed as diagnostic of the network structure of our samples include the following. (1) Melting points and glass transition values are high, but nonetheless lower than that of the completely polymerized CA network. (2) Raman spectra show only orthophosphate PO_4 in the glass. (3) As shown in Fig. 4 of reference nine and discussed further in section IVB, NMR spectra of ^{27}Al exhibit primarily fourfold Al–O coordination of Al, especially at lower $LaPO_4$ content. This implies that Al is a network former, not a modifier (as can sometimes be the case). These three observations lead us to conclude that the pattern of the samples' networks is consistent with their description as disrupted aluminate glasses, containing intercalated single phosphate groups.

3.4. Locations of ions: dissolution results

If we now ask where the metal ions in the networks are located, we may still draw on the above information but consider additional data from two sources: electron microprobe analysis following water treatment of the sample surface, and NMR. As noted in Section 2, our dissolution study arose from inappropriate sample preparation for microprobe analysis. Soaking the samples in water for approximately 1 h was found to remove all phosphate from the analyzed surface. This loss had a significant side effect, however, in that it was always accompanied by a proportional lanthanum loss. Mole for mole, the two ions always dissolved away together, indicating their close association in the sample.

3.5. NMR results for ^{31}P: spectra

The ^{31}P NMR spectra for our quenched glassy samples are characterized by a strong, broad feature near 0 ppm. The spectrum is directly deconvolutable into two lines: a relatively narrow peak at +2 ppm and a broader one at about −4 ppm (see Fig. 11 below and also reference nine).

Similar ^{31}P spectra were found for all $LaPO_4$-containing samples, with the exception of C12A7 75% $LaPO_4$, where an additional weak shoulder appears at more negative chemical shift values. In aluminophosphate glasses these two peaks would indicate the presence of orthophosphate (Q^0) species with either 1 or 2 s neighbor metal atoms.[23,24,19] The 75% sample's prominent shoulder may however also arise from Q^1 phosphates, i.e. phosphate groups with one (and only one) more phosphate as a second-nearest neighbor, in addition to an aluminum atom. This motivated further investigation of the question of P/Al proximity using the NMR TRAPDOR experiment, the findings from which are given next.

3.6. Results for ^{31}P/^{27}Al: double resonance (TRAPDOR)

As seen in Fig. 12, at both low and high ^{27}Al RF power a CA sample containing 27% $LaPO_4$ shows a very strong TRAPDOR response after 4 and 5 ms pulses of irradiation. When compared with results from other investigations,[21] this level of interaction implies that a large fraction of the phosphorus atoms are in close proximity to aluminum, i.e. as second-nearest neighbors, less than 4 Å distant. No TRAPDOR experiments have been attempted to date with the ^{139}La nucleus, whose NMR observation is difficult in many solid oxides.

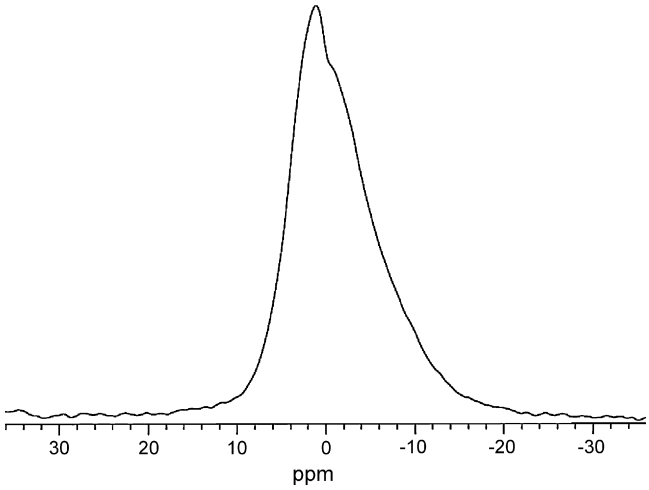

Fig. 11. ^{31}P MAS NMR spectrum of quenched $C_{12}A_7$:50% $LaPO_4$, showing two broad peaks in the vicinity of 0 ppm, separated by approximately 6 ppm. (Expanded from the spectrum shown in Fig. 5 of reference[9], erroneously identified therein as a 25% $LaPO_4$ sample spectrum.)

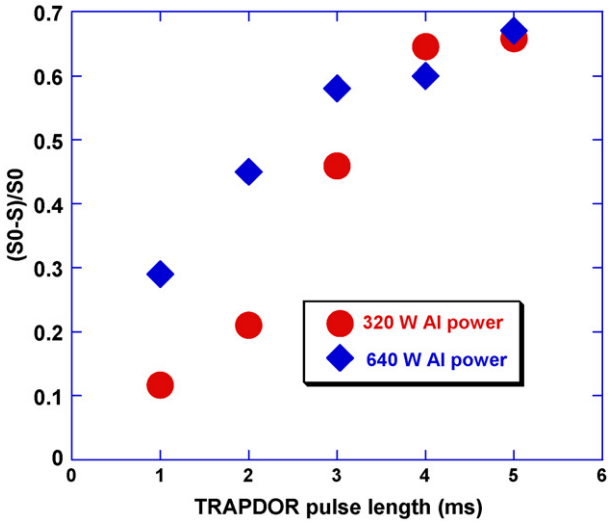

Fig. 12. TRAPDOR NMR: the sample is: 27% $LaPO_4$ in CA. Circles: ^{27}Al power pulsed at 320 W. Diamonds: Al power pulsed at 640 W.

3.7. Tabulation of NMR and T_g, T_m results

A full listing of the principal thermal and NMR properties of the samples is given in Table 3.

4. Discussion

4.1. Hydration of samples

Although the refractory reaction products of this system are generally non-reactive, they are well known for hydrat-

ing and binding large quantities of water.[15,16,26] Non-cement components of a mixture, such as lanthanum and phosphorus oxides, may hydrate at the sample surface. Lanthanum aluminate ($LaAlO_3$), and $LaPO_4$ are non-reactive with water, however they also may hydrate at low temperatures under normal conditions. Water of hydration is taken on by the aluminum nucleus in many compounds as a coordination partner, converting 4- and 5-coordinate aluminum to 6-coordinate.

The drop-quench into water for production of amorphous beads for NMR analysis was accordingly expected to yield a fully hydrated sample. However, Raman spectra and X-ray powder diffraction patterns of preheated or non-desiccated samples revealed them to be anhydrous, for both crystalline and glassy beads. Presumably, this surprising character of the bulk freshly quenched material is due to rapid initial hydration of the surface layers of a droplet. Such hydration would result in a thin outer shell that quickly becomes water-impermeable calcium aluminate cement, while the remaining bulk of the droplet cools to glass or crystal under effectively anhydrous conditions.

4.2. Glass structure in the $CaO–La_2O_3–Al_2O_3–P_2O_5$ system: incorporation of $LaPO_4$

In the absence of CaO, the remaining components up to 25% $LaPO_4$ of this system ($La_2O_3–Al_2O_3–P_2O_5$) are barely within the glass forming region.[4] Higher proportions of $LaPO_4$ would not be expected to form glasses. However, the CaO present in our system is a potent network modifier. Moreover, since Ca^{+2} could be expected to compete with La^{+3} for charge-balancing sites in the phosphorus–aluminum oxide network, the variations observed in glass forming profiles of the ternary system with $LaPO_4$ content could be expected. Our experimental findings, combined with known characteristics of aluminate and phosphate glasses, allow us to infer several basic structural features of our samples. We have incorporated these into structural models that represent average arrangements of the ions, including both network formers and modifiers. The models are based upon known bond lengths and angles, to the degree appropriate for a glass. An example will be given, following a brief review of the salient features upon which the models are based.

First, as noted above from the ^{27}Al NMR chemical shifts (Table 3), the Al ions are largely in 4-coordination to oxygen, although 5- or 6-coordinate aluminum is found at higher $LaPO_4$ content. Table 4 lists some estimated fractions of 4-coordinated Al in the samples vs. composition. Note however that the 50% $LaPO_4$ sample of the C12A7 series exhibits a dramatic shift away from 4- to 5-coordinate and most likely, 6-coordinate aluminum.

These results are in agreement with the widely held view of the short range structure expected of networks based upon that of pure calcium aluminate [CA] glass, namely as an assemblage of $(AlO_4)^-$ tetrahedra in a strongly inter-linked (corner-sharing) network, charge balanced by Ca^{2+} ions.[27] It is not surprising that CA, with a stoichometric ratio of Ca^{+2} to $(AlO_4)^-$ tetrahedra, has the highest T_g of our samples (~905 °C), while C12A7, with an excess of CaO acting as a network modifier breaking up the aluminate network, has a lower T_g of ~850 °C.[1,27] The addition of 50% $LaPO_4$ to C12A7 drops the T_g still more to ~812 °C, evidence of further breakup of the aluminate network and consistent with our Raman scattering results. The disruption may be attributable to the PO_4^{3-} ions forming terminal members of aluminate chains or nets. Water dissolution results then require that a lanthanum ion must be strongly linked to the terminal PO_4^{3-}. In this structure, the lanthanum cation would satisfy its high-coordination number preference[28] by being the center of a "ball" of calcium aluminate "nets". Phosphorus must also be coordinated closely with aluminum, according to our P/Al TRAPDOR findings.

Table 4
Estimated per cent 4-coordinate aluminum (Al^{IV}) in samples, based on ^{27}Al NMR chemical shift

Glass	
Sample	Al^{IV} (%)
C12A7	100
C12A7, 25% $LaPO_4$	89–94
C12A7, 50% $LaPO_4$	0
C12A7, 75% $LaPO_4$	N.A.
CA	80–89
CA, 25% $LaPO_4$	74–85
CA, 50% $LaPO_4$	49–71
CA, 75% $LaPO_4$	N.A.

Raman and MAS-NMR ^{31}P data, the latter especially indicating the association of La and Al with phosphate for all samples, are consistent with the presence of single phosphate tetrahedra intercalated into the aluminate network. Each tetrahedron is thus linked to one lanthanate tetrahedron and either one or two aluminate tetrahedra. As the starting $LaPO_4$ content increases towards 50%, the aluminate network makes a strong structural change, as seen in the increase from 4- to 6-coordination in Al chemical shift. However, the matrix of aluminate tetrahedra basically remains, the lanthanum orthophosphate groups being dispersed throughout. Based upon all of these considerations, we propose two somewhat different models for glass structures at low and high $LaPO_4$ content, as follows:

Structure of $LaPO_4$-containing samples with lower proportions of $LaPO_4$, leaving an intact alumina network: C12A7 series <25% $LaPO_4$, CA series <50% $LaPO_4$.[9]

Every lanthanum cation is linked (via an oxygen) to one phosphorus cation, on average, as in Fig. 13. Linkages of phosphate tetrahedra are rare and not larger than 2 units. A tetrahedral alumina network remains to a considerable extent, although it is not visible in either NMR or Raman spectra.

Phosphate is only present as orthophosphate or Q^0 species, not forming any chains, and is linked by bridging oxygen to at least one but no more than two aluminum cations. We have found in fact that all structural models constructed have at least one Al–O–P bond, supporting our inference that the chemical shift value range (0–2 ppm) for the principal ^{31}P line in the samples' NMR spectra is the result of P bonding with two near-neighbor metal ions, $La^{3+}$and Al^{3+}. It is also consistent

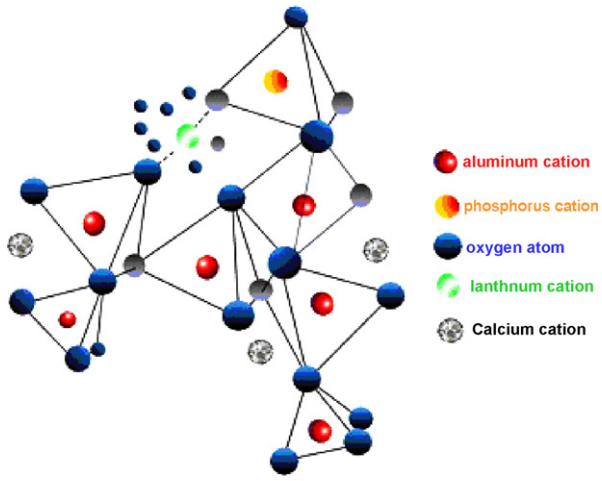

Fig. 13. Illustration of a possible lanthanum phosphate–calcium aluminate glass structure for lower LaPO4 content in calcium aluminate, derived from Raman and NMR data. For clarity, only a segment of the network is portrayed, with some oxygen atoms removed from the diagram.

with the NMR TRAPDOR results, showing close proximity between Al and P for most phosphorus atom.

Structure of $LaPO_4$-containing samples with sufficient $LaPO_4$ to completely disrupt the alumina network: C12A7 >25% $LaPO_4$, C12A7 >50% $LaPO_4$.

Linkages of phosphate tetrahedra are again not detected. We infer from Raman and ^{27}Al TRAPDOR NMR that the alumina groups are rarely linked together, but are always in association with Ca^{+2}, La^{+3}, or P^{+5} cations. The aluminum cations may now have a four-, five-, or sixfold coordination with oxygen, the last being prevalent.

5. Conclusion

A new protocol for synthesis of aluminates using hydrated $LaPO_4$ was developed. Studies of samples produced by addition of $LaPO_4$ to calcium aluminates led to the determination of a minimum melting temperature. Analysis of the resulting glassy samples indicates that La^{+3} ions never fully dissociate from the PO_4^{-3} ions, the two remaining in coordination with each other at all compositions. Ca^{2+}, a well-known modifier, is required to establish an aluminate tetrahedral network and form glasses, but $LaPO_4$ added to either CA or C12A7 acts to disrupt the network and is not a network former. Fourfold Al–O coordination is prevalent at lower $LaPO_4$ fractions, changing to six at higher ones (see $0.5LaPO_4{\cdot}0.5$ C12A7 glasses). NMR and Raman show PO_4^{3-} as orthophosphate units in all glasses, coordinated to one La and one or two Al second neighbor ions. At high $LaPO_4$ content, some quenched samples show the presence of the crystalline double phosphate $Ca_3La(PO_4)_3$.

Acknowledgements

This research was supported by the National Science Foundation through grant number DMR01-16361, and also by the Air Force Office of Scientific Research through grant numbers F4962-03-1-0346 and FA955004101153. We also wish to acknowledge early support by the Research Corporation, under grant number RA-0276. We thank P.F. McMillan and R. Weber for numerous helpful discussions and comments.

References

1. Higby, P., Ginther, R., Aggarwal, I. and Friebele, E., Glass formation and thermal properties of low-silica calcium aluminosilicate glasses. *Journal of Non-Crystalline Solids*, 1990, **126**, 209–215.
2. Mishra, K., Osterloh, I., Anton, H., Hannebauer, B., Schmidt, P. and Johnson, K., Electronic structures and host excitation of $LaPO_4$, La_2O_3, and $AlPO_4$. *Journal of Materials Research*, 1997, **12**, 2183–2190.
3. Keller, K., Mah, T.-I., Parthasarathy, T., Boakye, E., Mogilevsky, P. and Cinibulk, M., Effectiveness of monazite coatings in oxide/oxide composites after long-term exposure at high temperature. *Journal of the American Ceramic Society*, 2003, **86**, 325–332.
4. Karabulut, M., Metwalli, E. and Brow, R., Structure and properties of lanthanum–aluminium–phosphate glasses. *Journal of Non-Crystalline Solids*, 2001, **283**, 211–219.
5. Metwalli, E. and Brow, R., Modifier effects on the properties and structures of aluminophosphate glasses. *Journal of Non-Crystalline Solids*, 2001, **289**, 113–122.
6. Shoji, K. and Yasui, I., Structures of RF_2–$AlPO_4$ glasses revealed by diffraction and MD calculations. *Journal of Non-Crystalline Solids*, 1994, **177**, 125–130.
7. Marshall, D., Davis, J., Morgan, P., Waldrop, J. R. and Porter, J., Properties of La–monazite as an interphase in oxide composites. *Zeitschrift fur Metallkunde*, 1999, **90**, 1048–1052.
8. Boucher, S. *Melt Structure in the Al_2O_3–CaO–$LaPO_4$ System Studied by Ultra High-Temperature ^{27}Al NMR and Raman Spectroscopy. M.S. Thesis*. Arizona State University, Tempe, AZ, 2005.
9. Boucher, S., Piwowarczyk, J., Marzke, R., Takulapalli, B., Wolf, G., McMillan, P. *et al.*, Melt and glass structure in the Al_2O_3–CaO–$LaPO_4$ system studied by ^{27}Al and ^{31}P NMR, and by Raman scattering. *Journal of the European Ceramic Society*, 2005, **25**, 1333–1340.
10. Coutures, J.-P., Massiot, D., Bessada, C., Echegut, P., Rifflet, J.-C. and Taulelle, F., Etude par RMN 27Al d'aluminates liquides dans le domaine 1600–2100 °C. *Comptes Rendus de l'Academie des Sciences Serie II*, 1990, **310**, 1041.
11. Piwowarczyk, J. *Aluminum-27 Nuclear Magnetic Resonance Study of Molten Aluminum-Bearing Oxides. M.S. Thesis*. Arizona State University, Tempe, AZ, 2001.
12. Marzke, R., Piwowarczyk, J., McMillan, P. and Wolf, G., Al motion in levitated, molten Al_2O_3 samples, measured by pulsed gradient spin echo ^{27}Al NMR. *Journal of the European Ceramic Society*, 2005, **25**, 1325–1332.
13. Averbuch-Pouchot, M. and Durif, A., *Topics in phosphate chemistry*. World Scientific Publishing Co., 1996.
14. Chandrasekaran, A. *Phosphorus Chemistry: Introduction*. http://chandrasekaran.tripod.com/intro.html.
15. Kerr, J. A., In *CRC handbook of chemistry and physics 1999–2000*, ed. D. R. Lide. CRC Press, Boca Raton, Florida, USA, 2000.
16. Chatterjee, A., An update on the binary calcium aluminates appearing in aluminous cements. In *Calcium aluminate cements*, ed. Mangabhai and Glasser. IOM Communications, 2001, pp. 37–76.
17. Pollmann, H., Mineralogy and crystal chemistry of calcium aluminate cement. In *Calcium aluminate cements*, ed. Mangabhai and Glasser. IOM Communications, 2001, pp. 79–108.
18. Jungowska, W., The system $LaPO_4$–Ca_3 $(PO_4)_2$. *Solid State Science*, 2002, **4**, 229–232.
19. Brow, R., Review: the structure of simple phosphate glasses. *Journal of Non-Crystalline Solids*, 2000, **263–264**, 1–28.
20. van Eck, E., Janssen, R., Maas, W. and Veeman, W., A novel application of nuclear spin–echo double-resonance to aluminophosphates and aluminosilicates. *Chemical Physics Letters*, 1990, **174**, 428.
21. Lang, D., Alam, T. and Bencoe, D., Solid-state 31P/27Al and 31P/23Na TRAPDOR NMR investigations of the phosphorus environments in

sodium aluminophosphate glasses. *Chemistry of Materials*, 2001, **13**, 420–428.
22. Poe, B., McMillan, P., Cote, B., Massiot, D. and Coutures, J., Structure and dynamics in calcium aluminate liquids: high-temperature 27 Al NMR and Raman spectroscopy. *Journal of the American Ceramic Society*, 1994, **77**, 1832–1838.
23. Schneider, J., Oliveira, S., Nunes, L. and Panepucci, H., Local structure of sodium aluminum metaphosphate glasses. *Journal of the American Ceramic Society*, 2003, **86**, 317–324.
24. Dollase, W., Merwin, L. and Sebald, A., Structure of $Na_{3-3x}Al_xPO_4$, $x=0$ to.5. *Journal of Solid State Chemistry*, 1989, **83**, 140–149.
25. Massiot, D., Taulelle, F. and Coutures, J.-P., Structural diagnostic of high temperature liquid phases by ^{27}Al NMR. *Journal de Physique Colloques C5*, 1990, **51**(Suppl. 18), 425.
26. Iuga, D., Simon, S., de Boer, E. and Kentgens, A., A nuclear magnetic resonance study of amorphous and crystalline lanthanum–aluminates. *Journal of Physical Chemistry B*, 1999, **103**, 7591–7598.
27. McMillan, P. and Piriou, B., Raman spectroscopy of calcium aluminate glasses and crystals. *Journal of Non-crystalline Solids*, 1983, **55**, 221–242.
28. Hoppe, U., Kranold, R., Stachel, D., Barz, A. and Hannon, A. C., *Journal of Non-crystalline Solids*, 1998, **44**, 232–234.